Optimal Number and Locations of Controllers in Two-Dimensional Frames Using Genetic Algorithm

Zabih Mehdipour [1*]

[1] *University of Minho, Guimarães, Portugal.*

Abstract:
In this study, an Active tendon control system is employed to reduce the dynamic responses of a two-dimensional frame. Different placement or arrangement of active tendons generates different structural responses. By means of optimization methods, the best placement and arrangement of controllers would be found, which leads to minimum dynamic responses and, eventually, the least cost of fabrication. To determine the number and arrangement of controllers in the two-dimensional frame that was considered both shear and non-shear manner, the genetic algorithm has been used, hence; to measure the controller force, four different algorithms, including Classic, Instantaneous, modal, and pole assignment has been applied, and a comparison has been carried out about the influence of these algorithms as the control algorithms. Furthermore, the time delay effect of the control force on the optimized number and locations of the controllers has been explored. Moreover, the effect of different responses of the structure, for instance, peak inter-story drift, absolute peak acceleration, or peak displacement as the variable of optimization equations, has been demonstrated. Besides, by examining different earthquake time histories and various levels of peak ground acceleration, in the structure case study, the influence of different dynamic loads was surveyed.

© 2024 University of Mazandaran

1. Introduction

Active control techniques have been developed to reduce structural damage and improve safety, meanwhile accepting design and performance restrictions under different seismic excitation or wind loads. A new approach has been opened to optimization problems by considering the construction and maintenance cost of building and installation as well as the cost of structure control.

The number and placements of controllers and control forces are essential parameters in optimization problems. In this regard, some restrictions, such as maximum displacement or acceleration, are usually imported into this problem. Discreteness in the nature of the control environment, discreteness in the number and location of controllers and sensors, the robustness of control devices, the non-linear pattern of actively controlled structures, and the multi-modality of systems are the most significant features of this design problem that should be solved in multi-level.

The problem of optimal number and placements of controllers has been studied by several researchers in different aspects such as optimization algorithm, variables,

the objective function, the design constraints, active control algorithm, actively controlled structures, etc. Some of the most practical controllers are active tendon mechanisms (ATM), smart material, and active tuned mass damper (ATMD) [1]. Pantelides and Cheng [2] proposed two optimal location indices, including a control energy performance index and a response performance index, in order to find optimal placements of controllers in two-dimensional (2D) frames. Li et al. [3] took into consideration the complicated optimal design problem of integrating the number of actuators and the configuration of the actuators by suggesting a multi-level genetic algorithm in conjunction with two control algorithms, linear quadratic regulator (LQR) and acceleration feedback control algorithm. This approach was detailed in the next study by formulating a three-level optimal design problem involving a two-level genetic algorithm conducted on 2D frames controlled by active tendon actuators [4]. In this regard, the integral mechanical energy of the system was minimized. Liu et al. [5] investigated the optimal position of actuators in tall buildings under different earthquake excitations using a genetic algorithm. A classified multi-step procedure has been repeated recently while solving this mixed Discrete-continuous multi-objective programming. Gao et al. [6]

applied a two-step method in the optimization of active bars placement of intelligent truss structures with maximization of dissipation energy due to control action. In addition to searching for the optimal number and locations of controllers, the optimization of the control force became a significant purpose [7]. Liu et al. [8] found the optimal locations of sensors and actuators in flexible controlled structures employing the proposed genetic algorithm and a developed spatial H_2 norm-based computational scheme as a control algorithm. Rao et al. [1] surveyed the optimal placement problem on seismically excited High-rise buildings with a Multi-start Meta-heuristic algorithm combining simulated annealing and tabu search. Güney and Eşkinat [9] took into account the issue of the optimal location for actuators and sensors in flexible structures by applying a computationally simple H_∞ controller and a Gradient-based unconstrained minimization. Nandy et al. [10] investigated optimal sensors/actuator placement in smart structures using an island model parallel genetic algorithm. Wang and Li [11] determined the optimal piezoelectric sensor/actuator placement of cable net structures by means of H2-norm measures. Vashist and Chhabra [12] studied the optimal placement of piezoelectric actuators on plate structures for active vibration control using a genetic algorithm. Bruant and Proslier [13] conducted research to find the optimal location of piezoelectric actuators for active vibration control of thin axially functionally graded beams.

In the present study, different approaches have been considered for solving the optimization problem of the number and Locations of controllers in 2D frames. Moreover, the performance of different control algorithms, Classic, Instantaneous, modal, and pole assignment, in optimizing the number and placements of controllers are compared. Furthermore, the influence of peak inter-story drift, absolute peak acceleration, and peak displacement as the objective function has been investigated. In addition, the effect of different peak ground accelerations (PGA) of a series of scaled earthquakes and the time delay effect of controllers through an integral transformation method on the optimized number and placements of controllers are taken into consideration. In all cases, the optimization process is carried out by the discrete genetic algorithm on a structure that is actively controlled by the active tendon.

2. Review of Active Control Algorithms

2.1. The Classic Algorithm

The governing equation of motion for a structure with n degrees of freedom subjected to dynamic loading $F_{dyn}(t)$ and counteracted by the control force $u(t)$ can be expressed as follows [14].

$$M\ddot{x}(t) + C\dot{x}(t) + Kx(t) = F_{dyn}(t) + Du(t)$$
$$x = [x_1, x_2, \dots, x_n]^T \tag{1}$$

where M, C, and K are $n\times n$ mass, damping, and stiffness matrices, respectively. Also, $x(t)$ represents $n\times 1$ displacement vector and D states $n\times m$ matrix describing the location of m controllers. The equation of motion is

converted into the steady-space form as the following equation:

$$\dot{z}(t) = Az(t) + Bu(t) + H(t)$$
$$z(0) = z_0$$
$$z(t) = \begin{bmatrix} x(t) \\ \dot{x}(t) \end{bmatrix},$$
$$A = \begin{bmatrix} 0 & I \\ -M^{-1}K & -M^{-1}C \end{bmatrix}, \tag{2}$$
$$H(t) = \begin{bmatrix} 0 \\ M^{-1}F_{dyn}(t) \end{bmatrix},$$
$$B = \begin{bmatrix} 0 \\ M^{-1}D \end{bmatrix}$$

In which $z(t)$ is $2n\times 1$ state vector and A, B, and H declare $2n\times 2n$ system matrix, $2n\times m$ control matrix, and $2n\times 1$ load vector, respectively. The optimal control force will be achieved as below if the quadratic objective function is minimized and Equation 2 is simultaneously satisfied.

$$J = \int_{t_0}^{t_f} [z^T(t)Qz(t) + u^T(t)Ru(t)] \, dt \tag{3}$$

That t_0 and t_f are usually assumed zero and bigger than the duration of seismic excitation, respectively. Moreover, Q shows a $2n\times 2n$ positive semi-definite weighting matrix for the state variable and R is an $m\times m$ symmetric positive definite weighting matrix for the control force. Optimized preceding integral leads to the following control force.

$$u(t) = Gz(t) \quad G = -0.5R^{-1}B^T Pz(t) \tag{4}$$

where G is the gain matrix. Also, P expresses the Riccati matrix that can be obtained by solving the following Riccati matrix equation:

$$PA - 0.5PBR^{-1}B^T P + A^T P + 2Q = 0 \tag{5}$$

2.2. The Instantaneous Algorithm

The Time-dependent performance index for the steady-space equation (Equation 2) is defined as follows [15]:

$$J(t) = z^T(t)Qz(t) + u^T(t)Ru(t) \tag{6}$$

The governing equation of motion is gained as the following formula by transforming Equation 2, which was expressed in the real steady space, to modal space and solving this new equation using different numerical methods, such as the regular fourth-order Runge-Kutta method or the Simpson method.

$$z(t) = Td(t - \Delta t) + \frac{\Delta t}{2}[Bu(t) + H(t)] \tag{7}$$

$$d(t - \Delta t) = e^{\Lambda \Delta t}T^{-1}\left\{z(t - \Delta t) + \frac{\Delta t}{2}[Bu(t - \Delta t) + H(t - \Delta t)]\right\} \tag{8}$$

$$\Lambda = T^{-1}AT \tag{9}$$

where T is a $2n\times 2n$ modal matrix whose columns comprise of eigenvectors of the A matrix. In addition, Λ is a diagonal matrix, including eigenvalues of the A matrix. Also, $e^{\Lambda \Delta t}$ is a diagonal matrix consisting of $e^{\lambda \Delta t}$ in the case of λ is supposed to be the eigenvalue of the A matrix. Moreover,

$d(t − \Delta t)$ describes all dynamic characteristics. If the closed-loop control algorithm is taken into account, the state variable and control force are achieved as below by minimizing the objective function (Equation 6), which is restricted to Equation 7.

$$z(t) = \left[I + \frac{\Delta t^2}{4} BR^{-1}B^T Q\right]^{-1}\left[Td(t − \Delta t) + \frac{\Delta t}{2}H(t)\right] \qquad (10)$$

$$u(t) = -\frac{\Delta t}{2}R^{-1}B^T Qz(t) \qquad (11)$$

2.3. The Optimal Modal Algorithm

The governing equation of motion mentioned in Equation 1 is converted to modal space through the following equation [16]:

$$x(t) = \phi q(t) \qquad (12)$$

where ϕ and q are an $n \times n$ modal matrix and an $n \times 1$ modal displacement vector, respectively. By applying the preceding equation to Equation 1, the modal space equation can be extracted through the following relationships:

$$\ddot{q}(t) + \text{diag}(2\xi_j\omega_j)\dot{q}(t) + \text{diag}(\omega_j^2)q(t) = V(t) + W(t) \qquad (13)$$

$$\text{diag}(2\xi_j\omega_j) = M^{*-1}C^*, \quad \text{diag}(\omega_j^2) = M^{*-1}K^* \qquad (14)$$

$$M^* = \phi^T M\phi = \text{diag}(m^*_j), \quad C^* = \phi^T C\phi = \text{diag}(c^*_j) \qquad (15)$$

$$K^* = \phi^T K\phi = \text{diag}(k^*_j), \quad V(t) = M^{*-1}\phi^T Du(t) = Lu(t) \qquad (16)$$

$$W(t) = M^{*-1}\phi^T F_{dyn}(t) = NF_{dyn}(t), \quad L = M^{*-1}\phi^T D \qquad (17)$$

$$N = M^{*-1}\phi^T I \qquad (18)$$

For practical considerations, only the first r modes are controlled. Then Equation 13 is rewritten as below:

$$\ddot{q}_c(t) + \text{diag}(2\xi_{jc}\omega_{jc})\dot{q}_c(t) + \text{diag}(\omega_{jc}^2)q_c(t)$$
$$= V_c(t) + W_c(t) \qquad (19)$$
$$j = 1,2,\dots r$$

$$V_c(t) = L_c u(t), \quad W_c(t) = N_c F_{dyn}(t)L_c = L_{r\times m}, \quad N_c = N_{r\times n} \qquad (20)$$

in which q_c shows a modal displacement vector that is dimensionally much smaller than q. The above equation is converted to the steady state by the equation:

$$\dot{z}_c(t) = Az_c(t) + Bu(t) + H(t) \quad z_c(0) = z_{c0}, \qquad (21)$$

$$z_c(t) = \begin{bmatrix} q_c(t) \\ \dot{q}_c(t) \end{bmatrix},$$
$$A = \begin{bmatrix} 0 & I \\ -\text{diag}(\omega_{jc}^2) & -\text{diag}(2\xi_{jc}\omega_{jc}) \end{bmatrix},$$
$$H = \begin{bmatrix} 0 \\ N_c \end{bmatrix},$$
$$B = \begin{bmatrix} 0 \\ L_c \end{bmatrix}$$

Consequently, the control force and the modal state variable can be acquired by the implementation of the optimal control theory that was formerly described.

2.4. The Pole Assignment Optimal Algorithm

The general formation of open-loop poles of a structural system can be written as below [17]:

$$\lambda_i = \xi_i\omega_i \pm j\omega_i\sqrt{1 - \xi_i^2}$$
$$i = \sqrt{-1}$$
$$i = 1,2,\dots,2n \qquad (22)$$

In the pole assignment algorithm, open-loop poles shift to predetermined poles. Hence, in the first phase, the equation of motion transfers to modal space, and then the poles of each mode separately move to arbitrary regions. The state vector converts to modal space using the following transformation:

$$z_r(t) = T_r^T z(t)T^T \epsilon R^{r*n},$$
$$z_r(t)\epsilon R^r,$$
$$r < n \qquad (23)$$

where matrix T consists of eigenvectors of a matrix. Besides, T_r declares the column of T associated with the two poles of λ_r which should be shifted. By implementing Equation 23 to Equation 2 and Equation 4, the steady-state and linear optimal control equations will be accessed as follows:

$$\dot{z}_r(t) = A_r z_r(t) + B_r u(t)$$
$$T_r^T A = A_r T_r^T,$$
$$B_r = T_r^T B \qquad (24)$$

$$u(t) = G_r z_r(t) \quad G = G_r T_r^T \qquad (25)$$

The performance index of the discrete system will change in the new modal space as below:

$$J_r = \int_{t_0}^{t_f}[z^T_r(t)Qz_r(t) + u^T(t)u(t)]dt$$
$$Q = T_r Q_r T_r^T \qquad (26)$$

Now, the shifting process of each pole is described in modal space for both real pole and complex conjugate pairs.

2.4.1. Shifting One Eigenvalue to the Desired Location

An eigenvalue λ should be shifted to the desired location μ. Thus, Equation 28 should be rewritten as follows [17]:

$$\dot{z}_r(t) = \lambda z_r(t) + B_r u(t) \tag{27}$$

The eigenvalue λ can be related to the desired location μ. According to the following relationship, matrix P is obtained by:

$$\mu = \lambda - B_r B_r^T P \qquad Or \qquad P = \frac{(\lambda - \mu)}{B_r B_r^T} \tag{28}$$

Moreover, the state weighting matrix will result by:

$$Q_r = -2\lambda P + P B_r B_r^T P \tag{29}$$

2.4.2. Shifting a Pair of Eigenvalues to the Desired Location

A complex conjugate pair is shifted to another complex conjugate pair as well as a real pair is shifted to either a desired complex conjugate pair or another real pair. Here, T_r consists of two columns of T connected with the two poles of λ_r that should be shifted. The open-loop matrix and input matrix are defined below [17]:

$$A_r = \begin{bmatrix} \alpha & \beta \\ -\beta & \eta \end{bmatrix},$$
$$B_r = \begin{bmatrix} a & b \\ c & d \end{bmatrix} \tag{30}$$

Afterward, two possibilities will happen. If $\alpha \neq \eta$ then the open-loop pair are complex conjugate and if $\alpha \neq \eta$ and $\beta = 0$ then a real pair should be shifted. μ is assumed to be a complex conjugate as follows:

$$\mu = [\alpha + i\beta \,;\, \alpha - i\beta] \tag{31}$$

Through the Brogan algorithm, the gain matrix is calculated as:

$$G_r = [(\mu^* I_2 - A_r)^{-1} {}^* B_r]^{-1} \tag{32}$$

3. Review of the Time Delay Compensation Using an Optimal Control Procedure

If the control force applies to a structure after a time delay, the general equation of motion is rewritten by considering the time delay effect as [18]:

$$M\ddot{x}(t) + C\dot{x}(t) + Kx(t)$$
$$= F_{dyn}(t) + Du(t - \lambda), \tag{33}$$
$$x = [x_1, x_2, \dots, x_n]^T$$

In the steady space, Equation 33 can be rewritten as below:

$$\dot{z}(t) = Az(t) + Bu(t - \lambda) + H(t) \tag{34}$$

By employing the following transformation to Equation 34, the standard form of the first-order differential equation without any time delay term is obtained as Equation 36.

$$Y(t) = z(t) + \int_{-\lambda}^{0} e^{-A(\eta + \lambda)} Bu(t + \eta) d\eta \tag{35}$$

$$\dot{Y}(t) = AY(t) + B(A)u(t) + H(t) \tag{36}$$

$$B(A) = e^{-A\lambda} B$$

If the original steady-state is stable and controllable, the control system defined in Equation 34 will be stable and controllable. As a result of using different control algorithms mentioned in prior parts, the standard form of the steady state will be solved, and the control force $u(t)$ and the response of the structure $Y(t)$ will be derived. To achieve to the real steady-state z(t), the integral term written in Equation 37 should be solved.

$$Z_0(t) = \int_{-\lambda}^{0} e^{-A(\eta + \lambda)} Bu(t + \eta) d\eta \tag{37}$$

This integral term can be calculated with the aid of the numerical equation written as follows:

$$Z_0(t) = \sum_{j=1}^{\left[\frac{delay}{dt}\right]+1} \left(e^{(-A*\Delta t*(j-1))} * \right.$$
$$\left. \sum_{k=1}^{\infty} \frac{(-A)^{k-1}\xi^k}{k!} * B * u_{\left(t/dt - \left(\left[\frac{delay}{dt}\right]+1-j\right)\right)} \right) \tag{38}$$

4. The Genetic Algorithm

The Genetic Algorithm (GA) is a stochastic optimization technique based on the process of natural selection that belongs to the evolutionary algorithm. This algorithm consists of several subsections, including population selection, fitness function, parent selection, crossover, mutation, and termination. The population is a subset of solutions in the current generation, which can also be defined as a set of chromosomes. A predefined goal function, which combines the main goal parameter, such as maximum displacement in structural problems and all restrictions, is calculated and then sorted according to the best results. A major part of the worst population is removed and regenerated using the crossover operator. Throughout the crossover stage, more than one parent is determined by implementing proportionate fitness selection, some of which have been mentioned in technical books are Roulette Wheel Selection, Stochastic Universal Sampling (SUS), Tournament Selection, Rank Selection, and Random Selection, nominated and one or more off-springs are produced through the genetic material of the parents. Finally, the mutation is applied to the latest sorted population. Several mutation operators have been suggested, including Bit Flip Mutation, Random Resetting, Swap Mutation, Scramble Mutation, and Inversion Mutation. The crossover and mutation that will be followed by calculating and sorting the cost function is repeated unless convergence makes the algorithm a termination. Convergence occurs when there has been no improvement in the population, an absolute number of generations has been gained, or the objective function value has reached a predefined value [19].

5. Finding the Optimal Number and Locations on a 2D Frame

5.1. Earthquakes Records

Thirty records were selected to analyze different masonry structures. All records are for soil groups C and D, according to ASCE/SEI 7-16 [20]. The magnitude of all

records is between 6.0 km and 7.0 km. The distance to the fault is within the range of 20 (km) - 40 (km). Besides, no near-fault motions with directivity effects are included. In the following table (Table 1), the characteristics of all records are provided.

Table 1. 30 earthquake records characteristics

No.	Earthquake Name	Year	Station Name	Magnitude	Distance (km)	Vs30 (m/sec)
1	Imperial Valley-06	1979	Superstition Mtn Camera	6.53	24.61	362.38 (D)
2	Imperial Valley-06	1979	Victoria	6.53	31.92	242.05 (D)
3	Victoria_ Mexico	1980	SAHOP Casa Flores	6.33	39.1	259.59 (D)
4	Irpinia_ Italy-01	1980	Rionero In Vulture	6.9	27.49	574.88 (C)
5	Irpinia_ Italy-02	1980	Rionero In Vulture	6.2	22.68	574.88 (C)
6	Coalinga-01	1983	Parkfield - Fault Zone 12	6.36	27.96	265.21 (D)
7	Coalinga-01	1983	Parkfield - Fault Zone 15	6.36	28	307.59 (D)
8	Coalinga-01	1983	Parkfield - Fault Zone 16	6.36	26.2	384.26 (C)
9	Coalinga-01	1983	Parkfield - Fault Zone 2	6.36	37.92	294.26 (D)
10	Coalinga-01	1983	Parkfield - Fault Zone 8	6.36	28.58	308.84 (D)
11	Coalinga-01	1983	Parkfield - Gold Hill 2E	6.36	31.85	360.92 (D)
12	Coalinga-01	1983	Parkfield - Gold Hill 3E	6.36	28.72	450.61 (C)
13	Coalinga-01	1983	Parkfield - Gold Hill 3W	6.36	38.1	510.92 (C)
14	Coalinga-01	1983	Parkfield - Stone Corral 2E	6.36	35.29	566.33 (C)
15	Coalinga-01	1983	Parkfield - Stone Corral 3E	6.36	32.81	565.08 (C)
16	Coalinga-01	1983	Parkfield - Vineyard Cany 1E	6.36	24.83	381.27 (C)
17	Coalinga-01	1983	Parkfield - Vineyard Cany 1W	6.36	27.72	284.21 (D)
18	Coalinga-01	1983	Parkfield - Vineyard Cany 2W	6.36	29.01	438.74 (C)
19	Coalinga-01	1983	Parkfield - Vineyard Cany 3W	6.36	30.91	308.87 (D)
20	Coalinga-01	1983	Parkfield - Vineyard Cany 4W	6.36	33.28	386.19 (C)
21	Morgan Hill	1984	Capitola	6.19	39.08	288.62 (D)
22	Morgan Hill	1984	Corralitos	6.19	23.23	462.24 (C)
23	Morgan Hill	1984	San Juan Bautista_ 24 Polk St	6.19	27.15	335.5 (D)
24	Morgan Hill	1984	San Justo Dam (R Abut)	6.19	31.88	543.63 (C)
25	N. Palm Springs	1986	Indio	6.06	35.34	307.54 (D)
26	N. Palm Springs	1986	Joshua Tree	6.06	23.2	379.32 (C)
27	Chalfant Valley-02	1986	Benton	6.19	21.55	370.94 (C)
28	Chalfant Valley-02	1986	Convict Creek	6.19	29.35	382.12 (C)
29	Chalfant Valley-02	1986	Mammoth Lakes Sheriff Subst.	6.19	34.92	529.39 (C)
30	San Fernando	1971	LA - Hollywood Stor FF	6.61	22.77	316.46 (D)

These records are taken into account using different approaches. First of all, these records, which have been scaled by ASCE/SEI 7-16, are exerted to the 2D frame. Furthermore, each record has been separately exerted on the structure with different peak ground accelerations to comprehend the influence of various PGA.

5.2. Features of the 2D Frame

An Eight-story, Three-bay frame (Figure 1) designed according to ANSI/AISC 360-16 code [21] is considered a numerical example to be analyzed for the determination of optimal number and placements of controllers assuming both the shear building model and detailed finite element model. In the simple shear building model, each story is lumped as a single degree of freedom element. The structural parameters of this building are demonstrated in

Table 2. The damping matrix derived from the Rayleigh technique [22] is presented in the following equation:

$$C = 0.5585M + 0.0029K \tag{39}$$

In the detailed finite element model, both beams and columns are modeled employing a two-node six degrees of freedom planar beam element. Moreover, mass and stiffness matrices are extracted by analyzing structures using a matrix analysis. Also, the damping matrix, which is taken by Rayleigh's technique, is shown as follows:

$$C = 0.2021M + 0.0011K \tag{40}$$

In the present study, it is supposed that just the linear range behavior of steel will be considered. The modulus of elasticity of steel is equal to $210 \ GPa$.
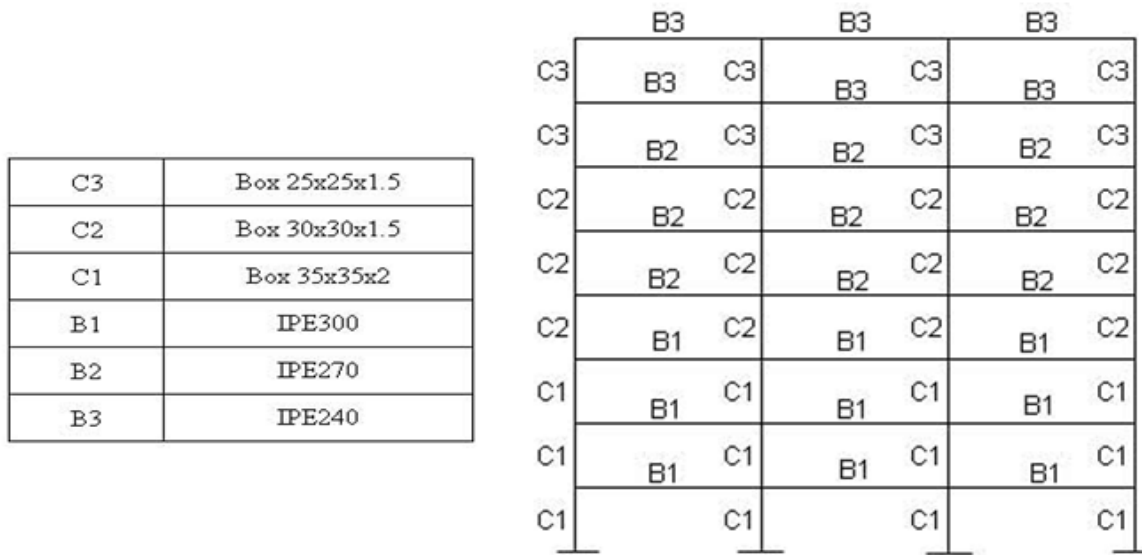
Figure 1. An eight-story Three-bay frame (right figure) and its members' characteristics (left figure)

Table 2. Structural matrices characteristics of the shear building model

Story	1	2	3	4	5	6	7	8
Mass (ton)	105.97	105.97	105.51	104.93	104.79	104.65	104.55	87.65
Stiffness ($1e8 * KN/m$)	2.136	2.136	2.136	2.136	2.136	2.136	2.136	2.136

5.3. Definition of the Optimization Problem

Different formulations have been considered while studying effective parameters in the optimal number and placements of controllers. The optimization problem can be defined for actively controlled structures under earthquake excitation as follows:

$$\begin{aligned} Goal\ function &= N_c + Coe_1 * drift_{max} \\ min \quad g_1 &= drift_{max} - drift_{all} \leq 0 \quad Coe_1 \ll 1 \\ g_2 &= (Con.f)_{max} - (Con.f)_{all} \leq 0 \end{aligned} \quad (41)$$

where N_c is the number of controllers placed in the structure. In addition, $drift_{max}$ and $(Con.f)_{max}$ state peak inter-story drift and control force, respectively. Moreover, $drift_{all}$ and $(Con.f)_{all}$ express allowable inter-story drift and control force, respectively. Also, Coe_1 declares a penalty multiplier. Optimal placements of controllers for a definite number of controllers are gained under dynamic loadings as below:

$$\begin{aligned} Goal\ function &= X_{max} \\ min \quad g_1 &= (Con.f)_{max} - (Con.f)_{all} \leq 0 \\ g_2 &= N_c - N_a = 0 \end{aligned} \quad (42)$$

in which X_{max} represents peak response, which is assumed to be displacement, absolute acceleration, and inter-story drift. Besides, N_a shows a predetermined number of controllers. It should be mentioned that in Equation 41, both the placements and the number of controllers are indefinite; however, in Equation 42, the number of controllers is definite, and the placements of controllers are desired.

In the current study, the both above formulations are taken into consideration. The number of variables and their possible quantities depends directly on the building behavior, which was classified as shear and non-shear

buildings in subsection 5.2. As previously mentioned, the optimization procedure is conducted by the genetic algorithm. It is noteworthy to remember that the number of columns in the population matrix is equal to the number of variables. Also, the number of rows is supposed to be 15 times the variable's number. Moreover, the number of variables is equal to the number of controllers, which is calculated based on all positions that a controller can be located. Consequently, for the shear frame, the number of variables is the same as the number of stories. Also, the non-shear frame is obtained from the number of stories multiplied by the number of bays. Additionally, for the shear frame, each variable changes from zero to the number of bays, and for the non-shear frame, it is either zero or one. In the crossover stage, firstly, 50 percent of the worst population is discarded and simultaneously regenerated among 50 percent of the best population. Parent selection is established based on the Roulette wheel selection procedure. Furthermore, the mutation coefficient is assumed to be 0.2.

5.4. Numerical Evaluation

In this subsection of the study, the results of the optimization process will be assessed and presented using different approaches. In all cases, 30 records presented in Table 1 are simultaneously exerted on the frame. However, for studying the influence of earthquake records, each record is separately applied. Also, under all circumstances, the classic algorithm (LQR) is conducted as the active control algorithm. However, for surveying the influence of different control algorithms, four algorithms explained in Subsection 2 will be considered.

Table 3 presents the optimal positioning of controllers for various numbers of controllers in the four control algorithms. In this case, by employing Equation 42 and supposing the peak inter-story drift as the cost function, the optimization problem for a specified number of controllers, which is assumed to be 3, 6, 9, 12, 15, and 18, would be solved. It should be mentioned that the peak inter-story drift is the average of peak inter-story drifts achieved by exerting 30 time-histories, demonstrated in Table 1, on the structure.

From the above table, it can be comprehended that the optimized arrangement of controllers, while using different control algorithms, is just slightly different and, in most cases, is negligible. Besides, in all cases, the number of assigned controllers in the lower half of the structure is more than in the upper half of it. The only exception generated in the instantaneous algorithm is that, in the case of using less than nine controllers, the controllers have been scattered almost equally between two halves of the structure. The other noticeable difference happens in the pole assignment algorithm. The number of controllers assigned to the lower half of the structure by using the pole assignment algorithm is considerably more than the respective achieved content by using other algorithms. Eventually, by ignoring these differences, it can be expressed that the optimized arrangement of the controllers is almost independent of the control algorithm.

In Table 4, the optimized number and arrangement of controllers by using different control algorithms and different peak ground accelerations of exerted time-histories are presented. It should be reminded that in this part, Equation 41 is conducted as the equation of optimization.

Based on Table 4, it is comprehensible that, by using modal and instantaneous algorithms, the least number of controllers is needed. Therefore, the best result is achieved by using these algorithms as the control algorithm, and by using the classic algorithm, the greatest number of controllers is allocated. Pondering on the results, it is comprehensible that the modal algorithm has better results in PGA's less than 1.2 g, and the instantaneous algorithm has better results in PGA's more than 1.2 g.

Furthermore, as implied before in Table 3, almost the balanced arrangement of controllers between the upper and lower half of the structure, by using the instantaneous algorithm, has the same pattern as this algorithm in this part.

It must be useful for the investigators to imply that during the process of the analysis, the processing time of the modal algorithm was considerably less than other algorithms. Hence, considering two significant issues, presenting the best results and the processing speed, the modal algorithm would be a perfect choice for the investigators to use, compared to the other three algorithms.

Tables 5 to 7 are showing the effect of the different cost functions. In this part, Equation 42 is used and the cost function (The x variable) is assumed to be peak inter-story drift, absolute peak acceleration and peak displacement, respectively.

Three proceeding Tables postulate that three variables, previously mentioned, have such similar results, especially, in the case that the number of possible controller increases. Furthermore, a pattern of filling the controllers in the structure is comprehensible. Initially, a controller will be located in a special bay from down to up and after filling the special bay, other bays respectively will be filled.

Table 8 demonstrates the effect of time delay on the optimal placements of controllers. Here, Equation 42 is taken into account, and the cost function is assumed to peak inter-story drift as well.

The results show that controllers are shifted to upper stories when time delay increases. The process of the positioning of controllers is similar to recent results.

Two following Tables show the effect of different records in optimal placements of controllers for 5 and 10 controllers. In this study, thirty earthquake records having equal PGA are separately exerted on the 2D frame and for determination of optimal placements of controllers, inter-story drift as a cost function should be minimized.

Tables 9 and 10 show that if different earthquake records that have equal PGA are exerted on the structure, the result of each record will be about equal. Perhaps this equality occurs in the range of earthquake records scaled following a specified code. Consequently, any general statement can be expressed by neglecting the frequency content and duration of the earthquake's occurrence.

Table 3. The optimal placements of controllers for different control algorithms

Algorithm	Number	Story							
		1	2	3	4	5	6	7	8
Classic	3	0	1	0	1	0	0	1	0
	6	1	1	1	1	0	1	0	1
	9	2	1	1	1	1	1	1	1
	12	2	2	2	2	1	1	1	1
	15	3	2	2	2	2	2	1	1
	18	3	3	2	2	2	2	2	2
Instantaneous	3	0	0	0	1	1	0	1	0
	6	1	1	0	1	1	1	1	0
	9	2	1	1	1	1	1	1	1

12	2	2	2	2	1	1	1	1
15	3	2	3	3	1	1	1	1
18	3	2	3	2	3	2	2	1
Modal								
3	1	1	0	1	0	0	0	0
6	1	1	0	1	1	1	1	0
9	1	2	2	1	1	1	1	0
12	2	2	2	1	1	1	1	2
15	2	2	3	2	2	2	1	1
18	2	2	3	2	2	2	3	2
Pole assignment								
3	0	1	0	1	0	1	0	0
6	2	1	0	1	1	0	1	0
9	2	1	1	1	1	1	1	1
12	2	2	2	2	1	1	1	1
15	3	3	3	2	1	1	1	1
18	3	3	3	3	1	1	1	3

Table 4. The optimal number of controllers for different control algorithms

		Story								
Algorithm	**PGA**	**1**	**2**	**3**	**4**	**5**	**6**	**7**	**8**	**Total number**
Classic	**0.6g**	1	0	0	0	0	0	0	0	1
	0.8g	1	1	1	0	0	0	0	0	3
	1g	1	0	1	1	1	1	0	0	5
	1.2g	1	1	1	1	1	1	0	0	6
	1.4g	2	1	2	1	1	1	1	0	9
	1.6g	2	2	1	2	1	1	1	0	10
	1.8g	2	2	2	2	1	1	1	0	11
	2g	2	3	2	2	2	1	1	0	13
Instantaneous	**0.6g**	0	0	0	1	1	0	1	0	3
	0.8g	0	0	0	1	1	0	1	0	3
	1g	0	0	0	1	1	1	1	0	4
	1.2g	1	0	0	1	1	1	1	0	5
	1.4g	1	1	1	1	1	0	1	0	6
	1.6g	2	1	0	2	1	1	1	0	8
	1.8g	2	2	2	2	1	1	1	0	11
	2g	3	2	1	3	2	1	1	0	13
Modal	**0.6g**	0	0	0	1	0	0	0	0	1
	0.8g	1	0	0	1	0	0	0	0	2
	1g	0	1	0	1	1	0	1	0	4
	1.2g	1	1	0	1	1	0	1	0	5
	1.4g	2	1	1	1	1	1	1	0	8
	1.6g	1	2	1	2	1	1	1	0	9
	1.8g	2	2	2	2	1	1	1	0	11
	2g	2	3	2	2	2	1	1	0	13
Pole assignment	**0.6g**	1	0	0	0	0	0	0	0	1
	0.8g	1	0	0	1	0	0	1	0	3
	1g	0	0	1	1	1	0	1	0	4
	1.2g	1	1	0	1	1	0	1	0	5
	1.4g	1	1	1	1	1	1	1	0	7
	1.6g	2	1	1	2	1	1	1	1	10
	1.8g	2	2	2	2	1	1	1	1	12

| **2g** | 2 | 2 | 2 | 2 | 2 | 1 | 1 | 1 | | 13 |

Table 5. The optimal placements of controllers by using peak inter-story drift as a cost function

Number of controllers	Story 1	Story 2	Story 3	Story 4	Story 5	Story 6	Story 7	Story 8
1	0	0	0	0	0	1	0	0
2	1	0	1	0	0	0	0	0
3	1	0	2	0	0	0	0	0
4	1	0	1	1	1	0	0	0
5	1	0	1	1	1	1	0	0
6	1	1	1	1	1	0	1	0
7	1	1	1	1	1	1	1	0
8	2	1	1	1	1	1	1	0
9	2	1	1	1	1	1	1	1
10	2	2	1	1	1	1	1	1
11	2	2	2	1	1	1	1	1
12	2	2	2	2	1	1	1	1
13	3	2	2	2	1	1	1	1
14	3	2	2	2	1	1	1	2
15	3	2	2	2	1	1	1	3
16	3	2	2	2	1	1	2	3
17	3	2	2	2	1	3	1	3
18	3	2	2	2	1	2	3	3

Table 6. The optimal placements of controllers by using absolute peak acceleration as a cost function

Number of controllers	Story 1	Story 2	Story 3	Story 4	Story 5	Story 6	Story 7	Story 8
1	0	0	0	0	0	0	1	0
2	0	0	0	1	0	0	1	0
3	0	1	0	1	0	0	1	0
4	0	1	1	1	0	1	0	0
5	0	1	1	1	1	0	1	0
6	1	1	1	1	0	1	0	1
7	1	1	1	1	1	1	1	0
8	1	1	1	1	1	1	1	1
9	2	1	1	1	1	1	1	1
10	2	2	1	1	1	1	1	1
11	2	2	2	1	1	1	1	1
12	2	2	2	2	1	1	1	1
13	2	2	2	2	2	1	1	1
14	2	2	2	2	2	2	1	1
15	3	2	2	2	2	2	1	1
16	3	3	2	2	2	2	1	1
17	3	3	2	2	2	2	2	1
18	3	3	2	2	2	2	2	2

Table 7. The optimal placements of controllers by using peak displacement as a cost function

Number of controllers	Story 1	Story 2	Story 3	Story 4	Story 5	Story 6	Story 7	Story 8

1	0	0	0	0	0	0	1	0
2	0	0	0	0	0	0	2	0
3	0	0	0	2	0	0	1	0
4	1	0	0	2	0	0	1	0
5	1	1	0	2	0	0	1	0
6	1	1	1	1	1	0	1	0
7	2	1	1	1	1	0	1	0
8	2	1	1	1	1	1	1	0
9	2	2	1	1	1	1	1	0
10	2	2	1	1	1	1	1	1
11	2	2	2	1	1	1	1	1
12	2	2	2	2	1	1	1	1
13	2	2	2	2	2	1	1	1
14	2	2	2	2	2	2	1	1
15	3	2	2	2	2	2	1	1
16	3	3	2	2	2	2	1	1
17	3	3	2	2	2	2	2	1
18	3	3	3	2	2	2	2	1

Table 8. The optimal placements of controllers for different time delays

Time delay (s)	Story 1	Story 2	Story 3	Story 4	Story 5	Story 6	Story 7	Story 8	Total number
0.05	0	1	0	1	0	1	0	0	3
0.05	1	1	0	1	1	1	1	0	6
0.05	2	2	1	1	1	1	1	0	9
0.05	2	2	2	2	1	1	1	1	12
0.1	0	0	0	1	1	0	1	0	3
0.1	0	0	1	2	1	1	1	0	6
0.1	1	1	2	1	2	1	1	0	9
0.1	1	3	2	1	2	1	1	1	12
0.15	0	0	0	0	1	2	0	0	3
0.15	0	0	1	1	1	1	1	1	6
0.15	2	0	1	2	1	1	1	1	9
0.15	2	2	2	2	2	1	1	0	12
0.2	0	0	0	1	1	1	0	0	3
0.2	0	0	1	1	2	1	1	0	6
0.2	0	0	1	3	3	1	1	0	9
0.2	1	3	2	1	2	1	1	1	12

Table 9. The optimal placements of 5 controllers for different earthquake records

Record number	Story 1	Story 2	Story 3	Story 4	Story 5	Story 6	Story 7	Story 8
1	1	1	0	1	1	1	0	0
2	1	1	0	1	1	1	0	0
3	1	1	0	1	1	1	0	0
4	1	0	0	1	1	1	1	0
5	1	1	0	1	1	1	0	0
6	1	1	0	1	1	1	0	0
7	1	1	0	1	1	1	0	0
8	1	1	0	1	1	1	0	0
9	1	1	0	1	1	1	0	0
10	1	1	0	1	1	1	0	0

11	1	1	0	1	1	1	0	0
12	1	1	0	1	1	1	0	0
13	1	1	0	1	1	1	0	0
14	1	1	0	1	1	1	0	0
15	1	1	0	0	1	1	1	0
16	1	1	0	1	1	1	0	0
17	1	1	0	1	1	1	0	0
18	1	1	0	1	1	1	0	0
19	1	1	0	1	1	0	1	0
20	1	1	0	1	1	1	0	0
21	1	1	0	1	1	1	0	0
22	1	1	0	1	1	1	0	0
23	1	1	0	1	1	1	0	0
24	1	0	0	1	1	1	1	0
25	1	1	0	1	1	1	0	0
26	1	1	0	1	1	1	0	0
27	1	1	0	1	1	1	0	0
28	1	1	0	1	1	1	0	0
29	1	1	0	1	1	1	0	0
30	1	1	0	1	1	1	0	0

Table 10. The optimal placements of 10 controllers for different earthquake records

Record number	Story 1	Story 2	Story 3	Story 4	Story 5	Story 6	Story 7	Story 8
1	2	2	1	2	1	1	1	0
2	2	2	2	1	1	1	1	0
3	2	1	1	1	2	2	1	0
4	2	2	1	2	1	1	1	0
5	2	2	1	1	1	1	1	1
6	2	2	1	1	1	2	1	0
7	2	2	1	1	1	1	1	1
8	2	2	1	1	1	1	1	1
9	2	2	1	1	1	1	1	1
10	2	1	1	1	2	2	1	0
11	2	1	1	1	2	2	1	0
12	2	2	2	1	1	1	1	0
13	2	2	1	1	1	2	1	0
14	2	2	1	1	1	1	1	1
15	2	2	1	2	1	1	1	0
16	2	2	1	1	1	1	1	1
17	2	2	1	2	1	1	1	0
18	2	2	1	1	1	2	1	0
19	2	2	1	1	1	2	1	0
20	2	2	1	2	1	1	1	0
21	2	2	1	1	1	1	1	1
22	2	2	1	2	1	1	1	0
23	2	2	1	2	1	1	1	0
24	2	2	1	1	1	2	1	0
25	2	2	1	1	1	1	1	1
26	2	1	1	1	2	2	1	0
27	2	1	1	1	2	2	1	0

28	2	1	1	1	2	2	1	0
29	2	2	1	2	1	1	1	0
30	2	2	2	1	1	1	1	0

6. Conclusions

In this paper, by using the genetic algorithm, the optimization problem of integrating the number and locations of the actuators in an 8-story and 3-span case study structure was studied with the trend of comparing the efficiency of four different control algorithms, including the classic algorithm, the modal algorithm, the instantaneous algorithm, and the pole assignment algorithm. Furthermore, the effect of the time delay of control forces, peak ground acceleration of exerted dynamic loads, and the elected response of the structure, as the variable of control equations, have been surveyed.

From the results of this study, the following conclusions are drawn:

i. The optimized arrangement of the controllers is almost independent of the control algorithm

ii. The optimized number of the allocated controllers by using the modal and instantaneous algorithms had the best results, and the classic algorithm had the worst results on this issue. If the processing time of the analysis is a matter of fact for researchers, the modal algorithm had the least process time compared to others. Thus, with regard to the best results in optimizing the number of controllers and less process time, the modal algorithm would be the best choice as the control algorithm.

iii. Election of the desired variable of the optimization equation (peak inter-story drift, absolute peak acceleration, peak displacement) will not significantly influence the optimized arrangement of controllers.

iv. The distribution of controllers at the height of the structure had better results under horizontal distribution in each story.

v. Vertical distribution of the controllers is mostly allotted to the lower levels of the structure, except in the instantaneous algorithm, where the controllers had been distributed almost equally in all stories.

vi. By increasing the time delay of the control force, the number of predicted controllers would increase, and more controllers would be assigned to the higher level of the structure.

vii. Earthquake time histories that have been normalized in the same pattern affect almost similarly to the optimized arrangement of the controllers.

7. References

[1] Rama Mohan Rao, A., & Sivasubramanian, K. (2008). Optimal placement of actuators for active vibration control of seismic excited tall buildings using a multiple start guided neighbourhood search (MSGNS) algorithm. Journal of Sound and Vibration, 311(1–2), 133–159. doi:10.1016/j.jsv.2007.08.031.

[2] Pantelides, C. P., & Cheng, F. Y. (1990). Optimal placement of controllers for seismic structures. Engineering Structures, 12(4), 254–262. doi:10.1016/0141-0296(90)90024-m.

[3] Li, Q. S., Liu, D. K., Fang, J. Q., & Tam, C. M. (2000). Multi-level optimal design of buildings with active control under winds using genetic algorithms. Journal of Wind Engineering and Industrial Aerodynamics, 86(1), 65–86. doi:10.1016/S0167-6105(00)00004-0.

[4] Li, Q. S., Liu, D. K., Tang, J., Zhang, N., & Tam, C. M. (2004). Combinatorial optimal design of number and positions of actuators in actively controlled structures using genetic algorithms. Journal of Sound and Vibration, 270(4–5), 611–624. doi:10.1016/S0022-460X(03)00130-5.

[5] Liu, D. K., Yang, Y. L., & Li, Q. S. (2003). Optimum positioning of actuators in tall buildings using genetic algorithm. Computers and Structures, 81(32), 2823–2827. doi:10.1016/j.compstruc.2003.07.002.

[6] Gao, W., Chen, J. J., Ma, H. B., & Ma, X. S. (2003). Optimal placement of active bars in active vibration control for piezoelectric intelligent truss structures with random parameters. Computers and Structures, 81(1), 53–60. doi:10.1016/S0045-7949(02)00331-0.

[7] Amini, F., & Tavassoli, M. R. (2005). Optimal structural active control force, number and placement of controllers. Engineering Structures, 27(9), 1306–1316. doi:10.1016/j.engstruct.2005.01.006.

[8] Liu, W., Hou, Z., & Demetriou, M. A. (2006). A computational scheme for the optimal sensor/actuator placement of flexible structures using spatial $\mathcal{H}2$ measures. Mechanical Systems and Signal Processing, 20(4), 881–895. doi:10.1016/j.ymssp.2005.08.030.

[9] Güney, M., & Eşkinat, E. (2008). Optimal actuator and sensor placement in flexible structures using closed-loop criteria. Journal of Sound and Vibration, 312(1–2), 210–233. doi:10.1016/j.jsv.2007.10.051.

[10] Nandy, A., Chakraborty, D., & Shah, M. S. (2019). Optimal Sensors/Actuators Placement in Smart Structure Using Island Model Parallel Genetic Algorithm. International Journal of Computational Methods, 16(6). doi:10.1142/S0219876218400182.

[11] Wang, Z., & Li, T. (2014). Optimal Piezoelectric sensor/actuator placement of cable net structures using H2-norm measures. JVC/Journal of Vibration and Control, 20(8), 1257–1268. doi:10.1177/1077546312472927.

[12] Vashist, S. K., & Chhabra, D. (2014). Optimal placement of piezoelectric actuators on plate structures for active vibration control using genetic algorithm. Active and Passive Smart

Structures and Integrated Systems 2014, 71. doi:10.1117/12.2044904.

[13] Bruant, I., & Proslier, L. (2016). Optimal location of piezoelectric actuators for active vibration control of thin axially functionally graded beams. International Journal of Mechanics and Materials in Design, 12(2), 173–192. doi:10.1007/s10999-015-9297-y.

[14] Soong, T. T., & Spencer, B. F. (1992). Active Structural Control: Theory and Practice . Journal of Engineering Mechanics, 118(6), 1282–1285. doi:10.1061/(asce)0733-9399(1992)118:6(1282).

[15] Yang, J.N., Akbarpour, A., Ghaemmaghami, P. (1987). Optimal Control Algorithms for Earthquake-Excited Building Structures. Structural Control, Springer, Dordrecht, Netherlands. doi:10.1007/978-94-009-3525-9_47.

[16] Fang, J. Q., Li, Q. S., & Jeary, A. P. (2003). Modified independent modal space control of m.d.o.f. systems. Journal of Sound and Vibration, 261(3), 421–441. doi:10.1016/S0022-460X(02)01085-4.

[17] Arar, A. R. S., & Sawan, M. E. (1993). Optimal pole placement with prescribed eigenvalues for continuous systems. Journal of the Franklin Institute, 330(5), 985–994. doi:10.1016/0016-0032(93)90089-D.

[18] Cai, G. P., Huang, J. Z., & Yang, S. X. (2003). An optimal control method for linear systems with time delay. Computers and Structures, 81(15), 1539–1546. doi:10.1016/S0045-7949(03)00146-9.

[19] Haupt, R. L., & Haupt, S. E. (2003). Practical Genetic Algorithms. John Wiley & Sons, Hoboken, United States. doi:10.1002/0471671746.

[20] ASCE/SEI 7-10. (2013). Minimum Design Loads for Buildings and Other Structures. American Society of Civil Engineers (ASCE), Reston, United States. doi: 10.1061/9780784412916.

[21] ANSI / AISC 360-16. (2016). Specification for Structural Steel Buildings. American Institute of Steel Construction (AISC), Chicago, United States.

[22] Clough, R. W., & Penzien, J. (1995). Dynamics of structures. McGraw-Hill College, New York, United States.